CHEMISTRY
A EUROPEAN JOURNAL

DOI: 10.1002/chem.201001613

Efficient Utilization of Higher-Lying Excited States to Trigger Charge-Transfer Events

Pierre-Antoine Bouit,[a] Fabian Spänig,[c] Gregory Kuzmanich,[d] Evangelos Krokos,[c] Christian Oelsner,[c] Miguel A. Garcia-Garibay,*[d] Juan Luis Delgado,[a, b] Nazario Martín,*[a, b] and Dirk M. Guldi*[c]

Dedicated to David I. Schuster on the occasion of his 75th birthday

Abstract: Several new fullerene–heptamethine conjugates, which absorb as far as into the infrared spectrum as 800 nm, have been synthesized and fully characterized by physicochemical means. In terms of optical and electrochemical characteristics, appreciable electronic coupling between both electroactive species is deduced. The latter also reflect the excited-state features. To this end, time-resolved, transient absorption measurements revealed that photoexcitation is followed by a sequence of charge-transfer events which evolve from higher singlet excited states (i.e., S_2—fast charge transfer) and the lowest singlet excited state of the heptamethine cyanine (i.e., S_1—slow charge transfer), as the electron donor, to either a covalently linked C_{60} or C_{70}, as the electron acceptor. Finally, charge transfer from photoexcited C_{60}/C_{70} completes the charge-transfer sequence. The slow internal conversion within the light-harvesting heptamethine cyanine and the strong electronic coupling between the individual constituents are particularly beneficial to this process.

Keywords: charge transfer · cyanines · dyes/pigments · excited states · fullerenes

Introduction

Natural systems that are able to efficiently transform sunlight into chemical energy through photosynthetic processes have inspired basic research and development into the areas of photovoltaics[1] and photocatalysis.[2] "Light" reactions, in which solar energy is harvested and converted into energy carriers, play a fundamental role in these processes. The successful mimicry of natural photosynthesis—involving a sequence of light-harvesting, light-funneling, charge-separation, and charge-shift processes—mandates the consideration of several aspects, broad light harvesting and efficient charge separation, combined with slow charge recombination.

For example, the delocalization of charges within the spherical carbon framework of C_{60}, together with the rigid, confined structure of its aromatic π sphere, offer unique opportunities for stabilizing charged entities. Above all, the small reorganization energies within fullerenes in charge-transfer reactions have led to a notable breakthrough in synthetic electron-donor–acceptor systems by providing accelerated charge separation and decelerated charge recombination. The vast majority of charge-transfer reactions com-

[a] Dr. P.-A. Bouit, Dr. J. L. Delgado, Prof. Dr. N. Martín
IMDEA-nanociencia, 28049 Madrid (Spain)

[b] Dr. J. L. Delgado, Prof. Dr. N. Martín
Departamento de Química Orgánica, Facultad de C. C. Químicas
Universidad Complutense de Madrid
28040 Madrid (Spain)
Fax: (+34) 91394-4103
E-mail: nazmar@quim.ucm.es

[c] F. Spänig, E. Krokos, C. Oelsner, Prof. Dr. D. M. Guldi
Department of Chemistry and Pharmacy &
Interdisciplinary Center of Molecular Materials (ICMM)
Friedrich-Alexander-University Erlangen-Nuremberg
Egerlandstr. 3, 91058 Erlangen (Germany)
Fax: (+49) 9131-85-28307
E-mail: dirk.guldi@chemie.uni-erlangen.de

[d] G. Kuzmanich, Prof. Dr. M. A. Garcia-Garibay
Department of Chemistry and Biochemistry, University of California
Los Angeles, California 90095-1569 (USA)
Fax: (+1) 310-825-0767
E-mail: mgg@chem.ucla.edu

Supporting information for this article is available on the WWW under http://dx.doi.org/10.1002/chem.201001613.

mence in energetically low-lying states. Ever since the pioneering work by Hammartström et al. on electron transfer from the higher-lying singlet excited states (i.e., S_2) of porphyrins to ruthenium(II) complexes,[3] follow-up studies on this topic have been published.[4] In these systems, the large energy gap existing between, for example, the higher-energy singlet excited states (i.e., S_2) and the lowest-energy singlet excited state (i.e., S_1), as well as the relatively long lifetime of S_2, emerged as key parameters. It has only been very recently that the possibility of designing optoelectronic switches has been suggested—relying upon electron-transfer events that are triggered from different excited state precursors in metal-containing porphyrins.[5]

On the other hand, only a few examples have been published of all-organic electron donors, involving aromatic-hydrocarbon-containing systems.[6] In this regard, the relationship between structure and charge-transfer reactivity will shape the efficiency of the conversion of solar power into energy, which makes it as important as any other parameter.

Light-harvesting ability, on the other hand, is a parameter that is rarely addressed, despite its paramount importance in organic photovoltaics. Extending the onset of light harvesting beyond 700 nm jeopardizes the charge-transfer efficiency by weakening the driving forces. Such a drawback can be partially compensated for by lowering the redox potential of the photoactive components, an alteration that is, however, often accompanied by chemical instability. This calls for higher-lying excited states as a precursor for nonadiabatic charge transfer.

In the context of light harvesting in the infrared section of the spectrum, the exceptional optical properties of heptamethine cyanines are a great asset. Their stability is based upon the delocalization of a positive charge between two terminal amino groups through a rigid, odd-numbered C(sp^2) skeleton.[7] The complex electronic structure of heptamethine cyanines results in structural inertia and, in turn, in slow structural relaxation/thermalization, especially of higher-energy excited states.[3b–d,4,8] All of the aforementioned criteria motivated us to probe these compounds as photo- and redox-active building blocks in conjunction with C_{60}, as well as C_{70}. Importantly—to the best of our knowledge—heptamethine cyanines covalently linked to fullerenes have never been probed in photoinduced charge-transfer reactions, either as the photo- or as the redox-active component.[9]

Herein, we report on uncommon charge-transfer evolutions from higher-energy singlet excited states of a heptamethine cyanine, as the electron donor, to a covalently linked C_{60} or C_{70}, as the electron acceptor. The slow internal conversion within the light-harvesting heptamethine and the strong electronic coupling between the individual constituents are beneficial to the process.

Results and Discussion

Synthesis: The syntheses of electron-donor–acceptor conjugates **2** and **3** were carried out in two steps starting from the previously described heptamethine cyanine **Cy**.[10] To this end, introducing *p*-hydroxybenzaldehyde to the chloro-heptamethine cyanine **Cy** was achieved by substitution of the *meso*-chlorine atom to form **1** (Scheme 1).[8a] The reaction of

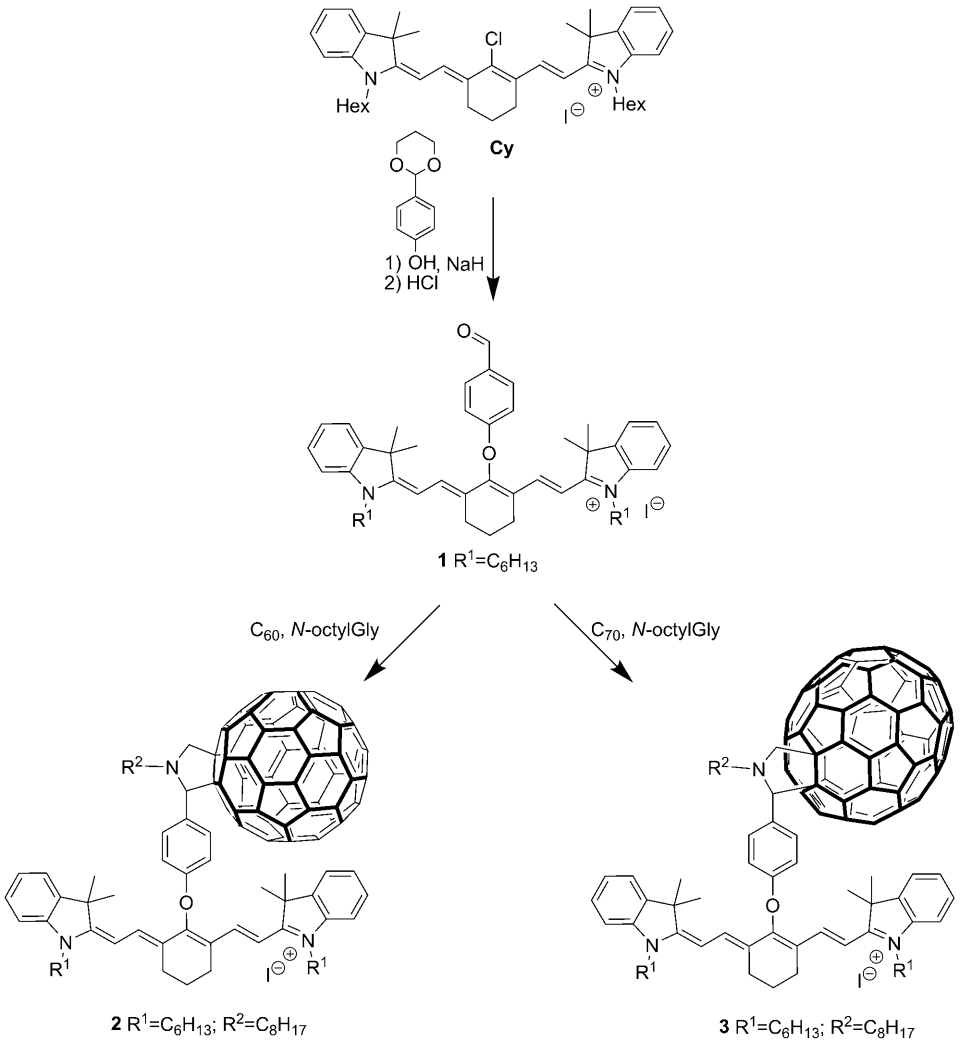

Scheme 1. The synthesis of fullerene–heptamethine conjugates **2** and **3**.

1 with either C_{60} or C_{70} in the presence of *N*-octylglycine[11] afforded **2** or **3** as deep green solids in 40 and 30% yields, respectively. Notably, **3** was obtained and studied as a mixture of isomers due to the multiple possible positions for adding azomethine ylides onto C_{70}.[12] The presence of various alkyl chains in **2** and **3** provides reasonable solubility to these compounds in common organic media. The structures of **2** and **3** were confirmed by ^{1}H and ^{13}C NMR spectroscopy and high-resolution MS experiments with molecular ion peaks for **2** $[M+H]^+$: 1555.6309 (calcd for $C_{118}H_{80}N_3O$: 1554.6296) and **3** $[M+H]^+$: 1675.6292 (calcd for $C_{128}H_{80}N_3O$: 1674.6301)—see Figures S1–S5 in the Supporting Information for details.

Optical properties: The absorbance of **1** has a maximum around 782 nm that is followed by weaker transitions in the blue region of the spectrum with maxima at 260, 387, and 440 nm (Figure 1). From this we calculated singlet excited-

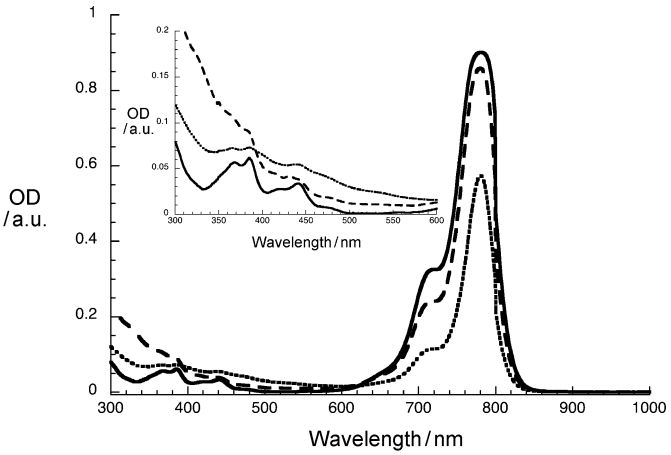

Figure 1. Absorption spectra of **1** (——), **2** (– – –), and **3** (•••••) recorded in dichloromethane (5.0×10^{-6} M).

state energies of ≈3.0 and 1.55 eV. The spectra of **2** and **3** resemble the sum of the individual spectra of **1** and either C_{60} or C_{70}. The well-known absorption bands of C_{60} and C_{70} are discernable at 256, 320, and 420 nm[13] and 236, 359, 377, 467, and 525 nm,[10,14] respectively. Evidence for electronic communication between the electron donor (i.e., **1**) and acceptor (i.e., C_{60} and C_{70}) units comes from the reduced extinction coefficients of **2** and **3** when compared to that of **1** (Figure 1).

Electrochemistry: The electrochemical properties of **1**, **2**, and **3** were studied in dichloromethane, at room temperature, by means of cyclic voltammetry (CV) and differential pulse voltammetry (DPV). As described for similar cationic heptamethines, **1** reveals an amphoteric redox character with a completely reversible one-electron reduction process at −1.02 V followed by a nonreversible reduction process at −1.94 V versus the ferrocene/ferricenium couple.[15] One-electron oxidation processes, on the other hand, are found at +0.30 V (fully reversible) and +0.93 V (quasi-reversible). Additionally, in **2**, three reversible one-electron reduction processes—all centered on C_{60}—were observed at −1.18, −1.52, and −2.07 V (Figure 2). In **3**, one-electron reduction

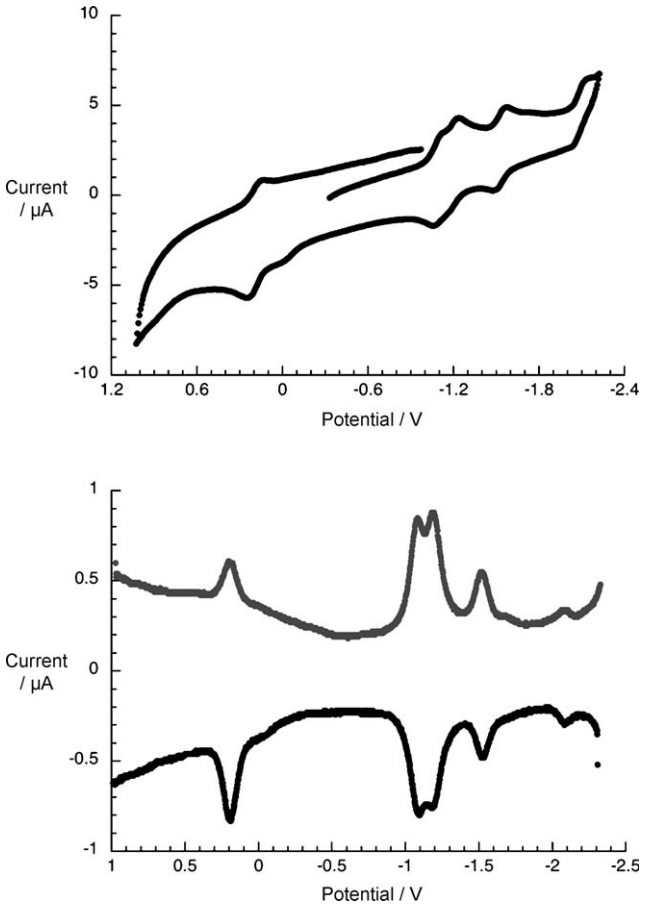

Figure 2. Top: cyclic voltammogram of **2**, recorded in deaerated dichloromethane versus the ferrocene/ferricenium couple—tributylammonium hexafluorophosphate ($TBAPF_6$) was employed as the supporting electrolyte. Bottom: the corresponding differential pulse voltammogram.

processes of C_{70} were detected at −1.20, −1.51, and −2.16 V. In comparison with pristine C_{60}, these reduction-potential values are cathodically shifted. Such a trend can be rationalized on the basis that a double bond of C_{60} has been saturated, which is known to raise the energy of the LUMO.[16,17] In both cases **2** and **3**, the first oxidation of the cyanine was shifted cathodically to +0.20 V without affecting the first reduction of **1**—see Figures S6 and S7 in the Supporting Information. Consequently, we derive radical-ion-pair state energies of 1.38 (**2**) and 1.4 eV (**3**) in dichloromethane.

Photophysical properties: Next, ultrafast laser flash photolysis experiments were carried out, employing either an excitation wavelength of 387 nm to mainly photoactivate C_{60} or C_{70} or an excitation wavelength of 775 nm to exclusively excite the cyanine moiety. Excitation of C_{60} and C_{70} at 387 nm populates their singlet excited states with character-

istic absorption maxima at 610/920[11b–18] and 610/1360 nm (Figure S8),[19] respectively. The latter undergo intersystem crossing to the corresponding triplet manifolds with characteristic lifetimes of between 0.7 and 1.4 ns and characteristic maxima at 700 nm.[11b,16,20] The transient absorption spectra upon 387 nm excitation of **1** (Figure S9 in the Supporting Information) in dichloromethane or benzonitrile are dominated by strong ground-state bleaching at 800 nm. Directly upon laser excitation, the higher-energy singlet excited state features of **1** are discernable due to maxima at 600, 850, and 940 nm, minima at 510, 565, 715, and 1255 nm, and broad bleach between 725 and 845 nm. With a lifetime of 2.6 ps, these features transform rapidly into those of the lowest-energy singlet excited state, with distinct maxima at 515, 560, and 1250 nm and distinct minima at 716 and 880 nm. The recovery of the ground state follows within 1650 ps. In contrast, if 775 nm excitation is used (Figure S10 in the Supporting Information) the lowest-energy singlet excited state (1.56 eV) is formed rapidly (<0.5 ps) bypassing any higher-energy singlet excited states, before converting into the triplet excited state.

When investigating **2** and **3**, the higher-energy singlet excited state features of **1** are discernable instantaneously upon photoexcitation at 387 nm—vide supra.[21] Considering the time window in which internal conversion and vibrational relaxation occurs within **1**, these transient characteristics in **2** and **3** start to transform, in benzonitrile, into the main maxima at 600, 1015, and 1050 nm (for **2**; Figure 3), as well as at 600, 850, 1015, and 1300 nm[11b,16,22] (for **3**)—the radical-ion-pair states. Support for this hypothesis was found by using a comparison with a spectroelectrochemically and pulse radiolytically generated radical dication of **1**. In fact, these are in perfect agreement with the transient maxima observed at 600 and 1050 nm. The transient features, on the other hand, at around 1015 and 850/1300 nm are in accordance with previous work that used pulse radiolysis and are assigned to the C_{60} and C_{70} radical anions, respectively.[23] Following the charge separation (k_{CS1}), the charge recombination (k_{CR}) to recover the ground state sets in with a lifetime of 30 ps for **2** (Figure 4) and 45 ps for **3** (Figure S11 in the Supporting Information).

The competition between charge transfer (k_{CS1}; i.e., 3.2 ps) and internal conversion/vibrational relaxation (i.e., 2.6 ps) is notable. The as-formed singlet excited states of **1** are discernable during the initial stages of our femtosecond experiments—shoulders at 515 and 560 nm and the 1250 nm maximum. The latter reveals shortened lifetimes (k_{CS2}) of 10 (**2**) and 14 ps (**3**) in benzonitrile, if compared with the intrinsic lifetime of **1**, to generate the same radical-ion-pair state that originated from the higher-energy singlet excited state (Figure 4). By decreasing the solvent polarity, the lifetimes for charge separation and charge recombination in **2** (Figure S12 in the Supporting Information) are extended to 3.5 and 14 ps, respectively. For **3**, the lifetimes are 3.5 and 175 ps. Such lifetimes suggest charge separation (i.e., k_{CS1}, k_{CS2}) and recombination (i.e., k_{CR}) dynamics that are in the normal and inverted region of the Marcus parabola, respectively. In fact, a correlation between the charge-transfer rate (i.e., charge separation and charge recombination) and the free-energy change for the underlying reaction reveals a parabolic dependence—as illustrated in Figure 5—with parameters of the reorganization energy (0.74 eV) and electronic coupling (89 cm^{-1}) closely resembling those seen in recent work involving C_{60}.[24]

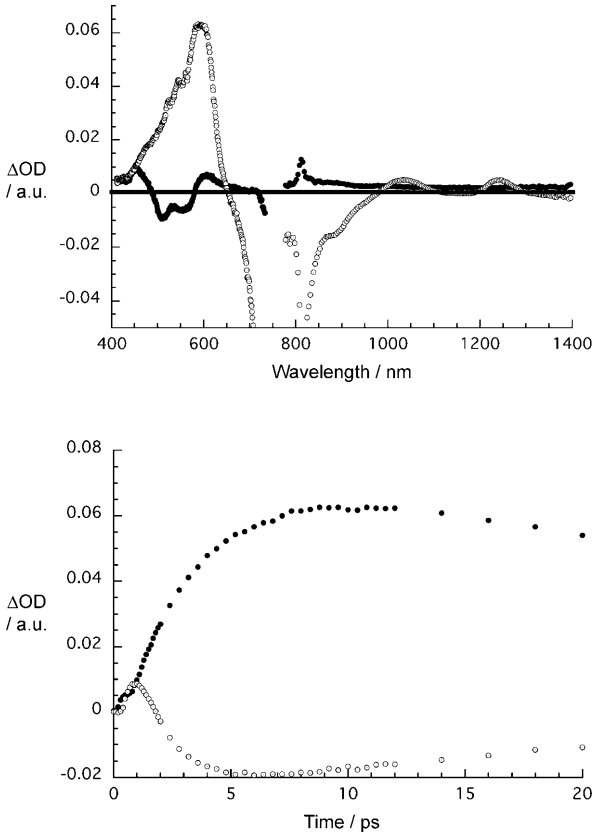

Figure 3. Top: differential absorption spectra (visible and near-infrared) obtained upon femtosecond flash photolysis (387 nm) of **2** in benzonitrile with two representative time delays between 0 and 10 ps at room temperature—time development is from ● to ○. Bottom: time–absorption profiles of the spectra shown in the upper part at 590 (●) and 855 nm (○) monitoring the competition between the formation of the singlet excited state and charge separation, as well as charge recombination.

When turning to the red area of the spectrum, the singlet excited state features of C_{60} or C_{70} are discernable. In the case of C_{70}, these evolve in a region beyond that of the heptamethine cyanine, 1350 to 1600 nm. Unlike those seen for the reference systems, the singlet excited-state features are short-lived and transform into those of the radical-ion-pair states—vide supra. Multiwavelength analyses provide lifetimes in dichloromethane of 9 ps for **2** and 11 ps for **3**.

Upon excitation of **2** (Figure 6) and **3** at 775 nm, the features of the directly and exclusively formed singlet excited state, that is, maxima at 515, 560, and 1250 nm, are, in contrast to **1**, short lived. In fact, they decay (k_{CS2}), in dichloromethane and benzonitrile, in 30 and 10 ps (**2**) and 21 and 14 ps (**3**) to the radical-ion-pair states. Spectroscopically, the latter comprise, for **2**, maxima at 600, 1015, and 1050 nm,

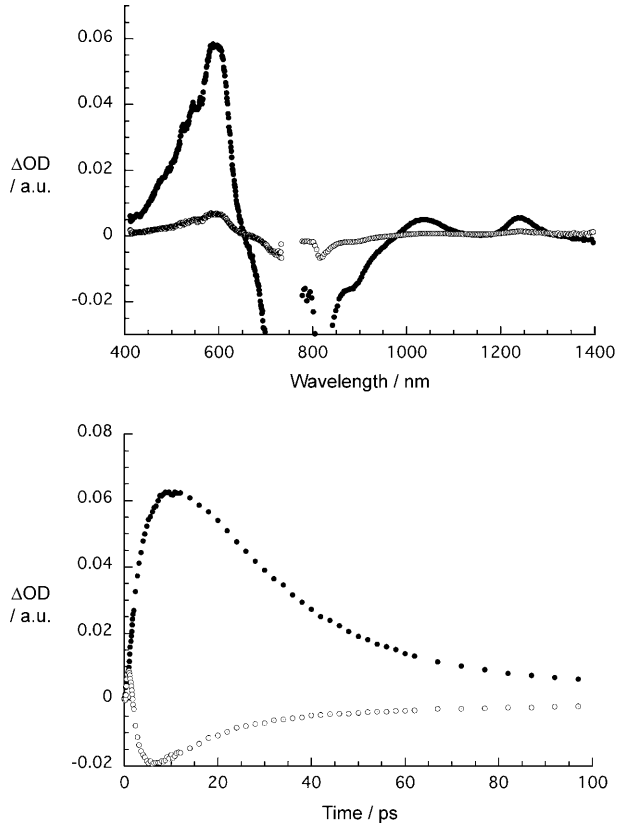

Figure 4. Top: differential absorption spectra (visible and near-infrared) obtained upon femtosecond flash photolysis (387 nm) of **2** in benzonitrile with two representative time delays between 0 and 100 ps at room temperature—time development is from ● to ○. Bottom: time–absorption profiles of the spectra shown in the upper part at 590 (●) and 855 nm (○) monitoring the charge separation and charge recombination.

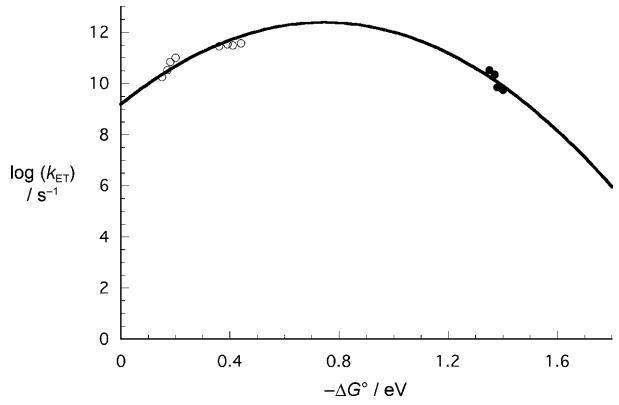

Figure 5. The dependence of the rate constants for charge separation (○) and charge recombination (●) on the driving force ($-\Delta G^0$).

whereas **3** exhibits maxima at 600, 850, 1015, and 1300 nm. The kinetic agreement is remarkably good—charge separation and charge recombination—between the 387 and 778 nm experiments.

In summary, photoexcitation of **2** or **3**, at 387 nm, with prompt formation of higher-energy singlet excited states results in two competing processes—Figure 7. On the one

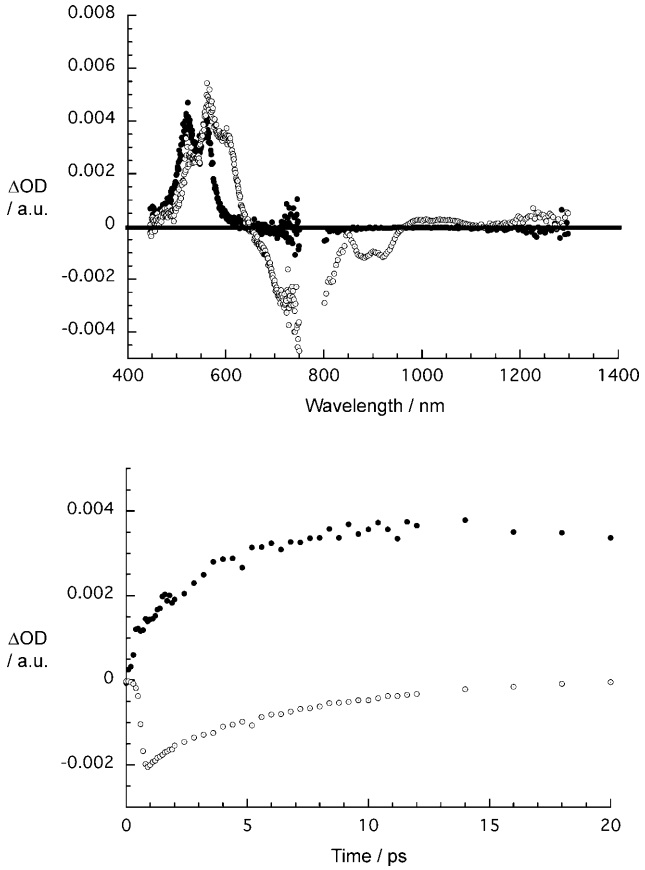

Figure 6. Top: differential absorption spectra (visible and near-infrared) obtained upon femtosecond flash photolysis (778 nm) of **2** in benzonitrile with two representative time delays between 0 and 10 ps at room temperature—time development from ● to ○. Bottom: time–absorption profiles of the spectra shown in the upper part at 590 (●) and 855 nm (○) monitoring the competition between the formation of the singlet excited state and charge separation, as well as charge recombination.

hand is the charge separation that occurs with driving forces around 1.5 eV. Key to this pathway is the small distance between the electron donor and the electron acceptor, which enables strong communication between them. On the other hand is the intrinsic deactivation to the lowest-energy singlet excited state, which is subject to a similar driving force. Considering the underlying kinetics, we estimate a branching of approximately 1:2 (i.e.; charge separation from heptamethine S_2:intrinsic deactivation $S_2 \rightarrow S_1$). From the lowest singlet excited state we observe a charge transfer that is about 10 times slower [$(k_{CS2}) = 30$ ps (**2**) and 21 ps (**3**), Table 1] than the charge transfer that finds its origins in the higher-energy singlet excited states [$(k_{CS1}) = 3.2$ ps (**2**) and 3.5 ps (**3**)]. Crucial for the slower kinetics are driving forces of about 0.15 eV. The higher-energy singlet excited-state energies of 1.79 (C_{60}) and 1.76 eV (C_{70}) accelerate the charge separation (k_{CS3}) by increasing the driving force to nearly 0.4 eV in dichloromethane in 9 ps (**2**). It also opens up new pathways for the recovery of the ground state, namely energy transfer.

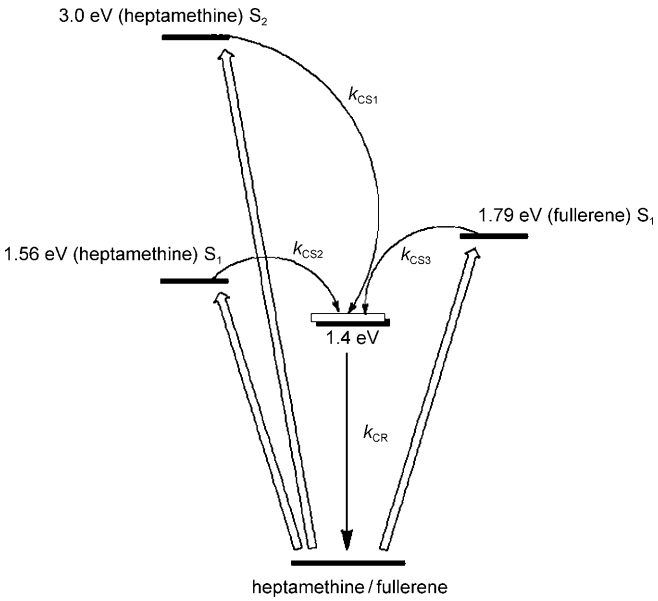

Figure 7. An energy diagram illustrating the different excitation, charge separation (k_{CS1}, k_{CS2}, k_{CS3}—see Table 1 for details), and charge recombination (k_{CR}) pathways of **2** and **3**.

Table 1. Charge separation and charge recombination rate constants for **2** and **3** in dichloromethane and benzonitrile.

	Solvent	k_{CS1} [10^{10} s^{-1}]	k_{CS2} [10^{10} s^{-1}]	k_{CS3} [10^{10} s^{-1}]	k_{CR} [10^{10} s^{-1}]
2	dichloromethane	28.6	3.33	11.1	0.71
	benzonitrile	31.3	10.0		3.33
3	dichloromethane	28.6	4.76	9.1	0.57
	benzonitrile	34.5	7.14		2.22

Conclusion

This investigation documents our success in realizing the rarely occurring scenario of a charge transfer commencing with a higher-energy excited state, through the careful choice of electron donor and electron acceptor. In particular, the slow internal deactivation of excited-state electron-donating heptamethine cyanine and the acceleration of charge-transfer reactions by the electron accepting C_{60}/C_{70} are crucial requisites. Currently, we are implementing heptamethine cyanines in multicomponent electron-donor–acceptor conjugates to slow down charge recombination. From a broader perspective, we hope that this finding will provide the impetus for breakthroughs in near-infrared responsive photovoltaic devices.

Experimental Section

General synthetic procedures: NMR spectra (^{1}H and ^{13}C) were recorded at room temperature on Bruker DPX 300 MHz or Bruker AVIII 500 MHz spectrometers. Data are listed in parts per million (ppm) and are reported relative to tetramethylsilane (^{1}H and ^{13}C) with residual solvent peaks being used as an internal standard (^{1}H: 7.26 ppm, $CHCl_3$; ^{13}C: 77.36 ppm, $CDCl_3$). High-resolution mass spectrometry measurements were performed at the Unidad de Espectrometría de Masas of Universidad Complutense de Madrid. Column chromatography was performed on Merck 60 (40–63 μm) silica. Compound **Cy** was prepared according to published procedures.[10b]

Synthesis of 1: 4-(1,3-Dioxan-2-yl)phenol (132 mg, 0.7 mmol, 1.1 equiv) was dissolved in DMF (20 mL), under an argon atmosphere and then NaH (19 mg, 1.2 equiv) was added. After 30 min of stirring at RT, this solution was added to **Cy** (500 mg, 0.66 mmol, 1 equiv) in DMF (20 mL). The solution was stirred for 6 h at RT and then poured into ice and hydrochloric acid (1 M, 200 mL). The resulting green solid was filtered off and dissolved in dichloromethane, and the resulting solution was washed with water. The organic phase was then dried with $MgSO_4$ and evaporated. The crude solid was then dissolved in the minimum amount of dichloromethane and precipitated in diethyl ether to afford a green solid (380 mg, 68 %). ^{1}H NMR (300 MHz, $CDCl_3$): $\delta = 0.9$ (t, $J = 7$ Hz, 6H), 1.1–1.5 (m, 14H), 1.63 (s, 12H), 1.7–1.8 (m, 4H), 2.0–2.1 (m, 2H), 2.7–2.8 (m, 2H), 4.12 (t, $J = 7$ Hz, 4H), 6.14 (d, $J = 15$ Hz, 2H), 7.05 (d, $J = 8$ Hz, 2H), 7.1–7.4 (m, 8H), 7.78 (d, $J = 15$ Hz, 2H), 7.97 (d, $J = 8$ Hz, 2H), 9.92 ppm (s, 1H); ^{13}C NMR (75 MHz, $CDCl_3$): $\delta = 4.9$, 14.0, 21.0, 22.5, 24.6, 26.7, 27.3, 27.9, 31.4, 44.9, 49.0, 100.7, 110.8, 115.4, 122.0, 122.1, 125.2, 128.7, 131.3, 132.7, 141.0, 141.2, 142.2, 162.3, 164.0, 171.9, 190.6 ppm: MS (ESI+): m/z: calcd for $C_{49}H_{61}N_2O_2$: 709.5 $[M]^+$; found: 709.6.

General procedure for the syntheses of 2 and 3: A solution of C_{60} or C_{70} (0.18 mmol, 3 equiv) and *N*-octylglycine (11 mg, 1 equiv) was refluxed in chlorobenzene (30 mL) for 30 min. Then, a solution of **1** (50 mg, 1 equiv) in chlorobenzene (10 mL) was added dropwise over 2 h. The solution was refluxed for a further 2 h and the solvent was evaporated off. The crude was purified by column chromatography on silica gel (eluent: toluene then CH_2Cl_2–MeOH, 9:1). The resulting product was dissolved in the minimum amount of dichloromethane and precipitated in pentane to afford a green solid.

Data for compound 2: Yield: 40 mg, 40 %; ^{1}H NMR (300 MHz, $CDCl_3$): $\delta = 0.9$ (t, $J = 7$ Hz, 9H), 1.1–1.5 (m, 36H), 1.7–1.8 (m, 6H), 2.0–2.1 (m, 2H), 2.4–2.6 (m, 2H), 2.7–2.9 (m, 4H), 3.0–3.1 (m, 1H), 4.12 (t, $J = 7$ Hz, 4H), 5.00 (s, 1H), 5.06 (d, $J = 9$ Hz , 1H), 6.10 (d, $J = 15$ Hz, 2H), 7.05 (d, $J = 8$ Hz, 2H), 7.1–7.4 (m, 8H), 7.85 ppm (d, $J = 15$ Hz, 2H); ^{13}C NMR (125 MHz, $CDCl_3$): $\delta = 14.4$, 14.5, 15.6, 21.1, 22.4, 22.6, 24.5, 26.6, 27.2, 27.8, 27.9, 28.0, 28.3, 29.4, 29.7, 31.4, 31.9, 44.8, 48.8, 48.9, 53.4, 65.8, 66.6, 67.3, 68.9, 76.6, 81.9, 100.3, 110.7, 121.9, 122.5, 125.0, 126.4, 128.2, 128.5, 128.7, 129.0, 129.6, 131.4, 134.2, 135.6, 136.0, 136.3, 137.2, 139.0, 139.8, 140.1, 140.2, 140.8, 141.2, 141.4, 141.5, 141.6, 141.7, 141.7, 141.8, 141.9, 142.0, 142.0, 142.1, 142.1, 142.2, 142.2, 142.3, 142.5, 142.5, 142.6, 142.7, 143.0, 143.1, 144.1, 144.3, 144.4, 144.7, 144.9, 145.0, 142.1, 145.3, 142.3, 145.3, 145.4, 145.5, 145.7, 145.8, 145.9, 146.0, 146.0, 146.1, 146.1, 146.2, 146.2, 146.3, 146.4, 146.5, 147.2, 147.3, 153.3, 153.4, 154.1, 156.6, 159.4, 163.5, 171.6 ppm; HRMS (MALDI+): m/z: calcd for $C_{118}H_{80}N_3O$: 1554.6296 $[M+H]^+$; found:1555.6309.

Data for compound 3: Yield: 30 %; HRMS (MALDI+): m/z: calcd for $C_{128}H_{80}N_3O$: 1674.6301 $[M+H]^+$; found: 1675.6292.

Electrochemistry: Electrochemical experiments were carried out by using a Princeton Applied Research Potentiostat/Galvanostat PAR 263 A. Cyclic voltammetry, differential pulse voltammetry and square-wave voltammetry were performed in a three electrode cell with a platinum wire as the counter electrode and a glassy carbon disk as the working electrode (Ø = 2 mm) versus a silver wire as the reference electrode; ferrocene was applied as an internal standard with a 0.1 M solution of $(t\text{Bu})_4NBF_4$ as the supporting electrolyte. All experiments were performed under inert-gas atmosphere and a compound concentration of 0.2 mM.

Spectroelectrochemistry: Spectroelectrochemical experiments were carried out by using a HEKA Elektronik Potentiostat/Galvanostat PG284 and a SPECORD S600 Analytic Jena Spectrophotometer. The measurements were performed in a homemade three-necked cell (≈0.3 cm) with platinum gauze as the working electrode and a platinum wire as the counter electrode versus a silver wire, under Argon atmosphere. Tetra-*n*-

butylammonium hexafluorophosphate (Bu_4NPF_6; 0.2 M) was used as the support.

Photophysics

Steady-state fluorescence spectroscopy: Spectra were collected by using a Horiba Jobin Yvon Fluoromax 3 spectrophotometer and in a deaerated solution, at room temperature (298 K), in a 1 cm quartz cuvette. All spectra were corrected for the instrument response. The monitoring wavelength corresponded to the maximum in the emission band.

Time resolved fluorescence spectroscopy: The fluorescence-lifetime measurements were performed by time correlated single photon counting (TCSPC) by using a FluoroLog-3 spectrometer in T-configuration (HORIBA-JOBIN YVON) including an MCP detector (R3809U-58). Fluorescence lifetimes were measured at the emission maximum, at room temperature, in a deaerated solution, in a 1 cm quartz cuvette.

Femtosecond transient absorption spectroscopy: Femtosecond transient absorption studies were performed with 775 and 387 nm laser pulses (1 kHz, 150 fs pulse width, 200 nJ) from an amplified Ti/sapphire laser system (Model CPA 2101, Clark-MXR Inc.—output 775 nm). The transient absorption pump probe spectrometer (TAPPS) Helios from Ultrafast systems is referred to as a two-beam setup, in which the pump pulse is used as the excitation source for transient species and the delay of the probe pulse is exactly controlled by an optical delay rail. As the probe (white light continuum), a small fraction of pulses stemming from the CPA laser system is focused by a 50 mm lens into a 3 mm thick sapphire disc. The transient spectra were recorded by using fresh, oxygen-free solutions for each laser excitation. All experiments were performed at 298 K, in a 2 mm quartz cuvette.

Pulse radiolysis: Pulse radiolysis experiments were performed by using 50 ns pulses of 15 MeV electrons from a linear electron accelerator (LINAC). Dosimetry was based upon the oxidation of SCN^- to $(SCN)_2^-$, which, in aqueous, N_2O-saturated solution, takes place with $G \approx 6$ (G denotes the number of species per 100 eV, or the approximate μM concentration per 10 J of absorbed energy). The radical concentration generated per pulse was varied between $(1–3) \times 10^{-6}$ M.

Acknowledgements

The Deutsche Forschungsgemeinschaft (Grant SFB 583), the Cluster of Excellence "Engineering of Advanced Materials", the FCI, and the Office of Basic Energy Sciences of the US Department of Energy are gratefully acknowledged. M. A. G.-G and G. K. acknowledge the NSF IGERT: Materials Creation Training Program (MCTP)—DGE-0654431 and grant NSF-CHE 0844455. This work has been supported by the European Science Foundation (SOHYD, MAT2006-28170-E), the MEC of Spain (CT2008-00795/BQU and Consolider-Ingenio 2010C-07-25200, Nanociencia Molecular), and the Comunidad de Madrid (MADRISOLAR-2, S2009/PPQ-1533). J. L. D. thanks the MICINN of Spain for a Ramón y Cajal Fellowship, co-financed by the EU Social Funds. P. A. B. thanks IMDEA-Nanociencia for a postdoctoral research grant.

[1] For some very recent special issues, see: a) Special issue on "Organic Photovoltaics": *Acc. Chem. Res.* **2009**, *42*, 1689, edited by J.-L. Bredas, J. R. Durrant; b) Special issue on "Renewable Energy": *Chem. Soc. Rev* **2009**, *38*, 1, edited by D. Nocera, D. M. Guldi; c) B. O'Regan, M. Grätzel, *Nature* **1991**, *353*, 737; d) S. Wenger, P.-A. Bouit, Q. Chen, J. Teuscher, D. Di Censo, R. Humphry-Baker, J. E. Moser, J. L. Delgado, N. Martín, S. M. Zakeeruddin, M. Grätzel, *J. Am. Chem. Soc.* **2010**, *132*, 5164; e) S. Günes, H. Neugebauer, N. S. Sariciftci, *Chem. Rev.* **2007**, *107*, 1324; f) B. C. Thompson, J. M. J. Frechet, *Angew. Chem.* **2008**, *120*, 62; *Angew. Chem. Int. Ed.* **2008**, *47*, 58; g) J. L. Delgado, P.-A. Bouit, S. Filippone, M. A. Herranz, N. Martín, *Chem. Commun.* **2010**, *46*, 4853; h) I. Riedel, E. von Hauff, J. Parisi, N. Martín, F. Giacalone V. Diakonov, *Adv. Funct. Mater.* **2005**, *15*, 1979.

[2] a) N. Armaroli, V. Balzani, *Angew. Chem.* **2007**, *119*, 52; *Angew. Chem. Int. Ed.* **2007**, *46*, 52; b) A. Fihri, V. Artero, M. Razavet, C. Baffert, W. Leibl, M. Fontecave, *Angew. Chem.* **2008**, *120*, 574; *Angew. Chem. Int. Ed.* **2008**, *47*, 564.

[3] D. LeGourriérec, M. Andersson, J. Davidsson, E. Mukhtar, L. Sun, L. Hammarstrom, *J. Phys. Chem. A* **1999**, *103*, 557.

[4] a) N. Mataga, H. Chosrowjan, Y. Shibata, N. Yoshida, A. Osuka, T. Kikuzawa, T. Okada, *J. Am. Chem. Soc.* **2001**, *123*, 12422; b) T. Kesti, N. Tkachenko, H. Yamada, H. Imahori, S. Fukuzumi, H. Lemmetyinen, *Photochem. Photobiol. Sci.* **2003**, *2*, 251; c) J. Petersson, M. Eklund, J. Davidsson, L. Hammarström, *J. Am. Chem. Soc.* **2009**, *131*, 7940.

[5] S. Wallin, C. Monnereau, E. Blart, J.-R. Gankou, F. Odobel, L. Hammarström, *J. Phys. Chem. A* **2010**, *114*, 1709.

[6] a) P.-A. Muller, E. Vauthey, *J. Phys. Chem. A* **2001**, *105*, 5994; b) M. Sakamoto, X. Cai, M. Hara, M. Fujitsuka, T. Majima, *J. Am. Chem. Soc.* **2004**, *126*, 9709.

[7] a) R. S. Lepkowicz, O. V. Przhonska, J. M. Hales, J. Fu, D. J. Hagan, E. W. Van Stryland, M. V. Bondar, Y. L. Slominsky, A. D. Kachkovski, *Chem. Phys.* **2004**, *305*, 259; b) P.-A. Bouit, C. Aronica, L. Toupet, B. Le Guennic, C. Andraud, O. Maury, *J. Am. Chem. Soc.* **2010**, *132*, 4328.

[8] a) R. S. H. Liu, A. E. Asato, *J. Photochem. Photobiol. C* **2003**, *4*, 179; b) N. Mataga, S. Taniguchi, H. Chosrowjan, A. Osuka, N. Yoshida, *Photochem. Photobiol. Sci.* **2003**, *2*, 493; c) M. Sakamoto, X. Cai, M. Hara, S. Tojo, M. Fujitsuka, T. Majima, *J. Phys. Chem. A* **2004**, *108*, 10941; d) M. Kubo, Y. Mori, M. Otani, M. Murakami, Y. Ishibashi, M. Yasuda, K. Hosomizu, H. Miyasaka, H. Imahori, S. Nakashima, *J. Phys. Chem. A* **2007**, *111*, 5136.

[9] For an example of systems with smaller trimethine cyanine and C_{60} showing weak photovoltaic properties, see: F. Meng, J. Hua, K. Chen, H. Tian, L. Zuppiroli, F. Nuesch, *J. Mater. Chem.* **2005**, *15*, 979.

[10] a) N. Narayanan, G. J. Patonay, *J. Org. Chem.* **1995**, *60*, 2391; b) P.-A. Bouit, G. Wetzel, G. Berginc, L. Toupet, P. Feneyrou, Y. Bretonnière, O. Maury, C. Andraud, *Chem. Mater.* **2007**, *19*, 5325.

[11] a) M. Maggini, G. Scorrano, M. Prato, *J. Am. Chem. Soc.* **1993**, *115*, 9798; b) M. Prato, M. Maggini, *Acc. Chem. Res.* **1998**, *31*, 519; c) N. Tagmatarchis, M. Prato, *Synlett* **2003**, 768.

[12] a) A. Hirsch, M. Brettreich in *Fullerenes*, Wiley-VCH, Weinheim, **2005**; b) J. L. Delgado, E. Espíldora, M. Liedtke, A. Sperlich, D. Rauh, A. Baumann, C. Deibel, V. Dyakonov, N. Martín, *Chem. Eur. J.* **2009**, *15*, 13474.

[13] a) S. Leach, M. Vervloet, A. Desprès, F. Bréheret, J. P. Hare, T. J. Dennis, H. W. Kroto, R. Taylor, D. R. M. Walton, *Chem. Phys.* **1992**, *160*, 451; b) D. M. Guldi, K.-D. Asmus, *J. Phys. Chem. A* **1997**, *101*, 1472.

[14] H. Ajie, M. M. Alvarez, S. J. Anz, R. D. Beck, F. Diederich, K. Fostiropoulos, D. R. Huffman, W. Krätschmer, Y. Rubin, K. E. Schriver, D. Sensharma, R. L. Whetten, *J. Phys. Chem.* **1990**, *94*, 8630.

[15] P.-A. Bouit, D. Rauh, S. Neugebauer, J. L. Delgado, E. Di Piazza, S. Rigaut, O. Maury, C. Andraud, V. Dyakonov, N. Martín, *Org. Lett.* **2009**, *11*, 4806.

[16] L. Echegoyen, L. E. Echegoyen, *Acc. Chem. Res.* **1998**, *31*, 593.

[17] a) N. Martín, L. Sanchez, B. Illescas, I. Perez, *Chem. Rev.* **1998**, *98*, 2527; b) N. Martín, *Chem. Commun.* **2006**, 2093; c) N. Martin, L. Sanchez, M. A Herranz, B. M. Illescas, D. M. Guldi, *Acc. Chem. Res.* **2007**, *40*, 1015; d) F. Giacalone, J. L. Segura, N. Martin, D. M. Guldi, *J. Am. Chem. Soc.* **2004**, *126*, 5340; e) M. A. Herranz, N. Martin, S. Campidelli, M. Prato, G. Brehm, D. M. Guldi, *Angew. Chem.* **2006**, *118*, 4590; *Angew. Chem. Int. Ed.* **2006**, *45*, 4478; f) M. Wielopolski, C. Atienza, T. Clark, D. M. Guldi, N. Martin, *Chem. Eur. J.* **2008**, *14*, 6379; g) S. S. Gayathri, M. Wielopolski, E. M. Perez, G. Fernandez, L. Sanchez, R. Viruela, E. Orti, D. M. Guldi, N. Martin, *Angew. Chem.* **2009**, *121*, 829; *Angew. Chem. Int. Ed.* **2009**, *48*, 815; h) A. Molina-Ontoria, G. Fernandez, M. Wielopolski, C. Atienza, L. Sanchez, A. Gouloumis, T. Clark, N. Martin, D. M. Guldi, *J. Am. Chem. Soc.* **2009**, *131*, 12218; i) B. M. Illescas, J.

Santos, M. Wielopolski, C. M. Atienza, N. Martin, D. M. Guldi, *Chem. Commun.* **2009**, 5374.
[18] D. M. Guldi, F. Hauke, A. Hirsch, *Res. Chem. Intermed.* **2002**, *28*, 817.
[19] C. S. Foote, *Top. Curr. Chem.* **1994**, *169*, 347.
[20] M. R. Fraelich, R. B. Weisman, *J. Phys. Chem.* **1993**, *97*, 11145.
[21] Approximate absorption ratio between C_{60}/C_{70} and the heptamethine cyanine is 9:1.
[22] C. A. Reed, R. D. Bolskar, *Chem. Rev.* **2000**, *100*, 1075.
[23] G. H. Sarova, U. Hartnagel, D. Balbinot, S. Sali, N. Jux, A. Hirsch, D. M. Guldi, *Chem. Eur. J.* **2008**, *14*, 3137.
[24] F. Spänig, M. Ruppert, J. Dannhäuser, A. Hirsch, D. M. Guldi, *J. Am. Chem. Soc.* **2009**, *131*, 9378

Received: June 8, 2010
Published online: July 26, 2010

